Available online at www.sciencedirect.com

SCIENCE DIRECT

Virology 338 (2005) 259 – 269

VIROLOGY

www.elsevier.com/locate/yviro

Neutralization of a common cold virus by concatemers of the third ligand binding module of the VLDL-receptor strongly depends on the number of modules

Rosita Moser[a,b,1], Luc Snyers[a,2], Juergen Wruss[a], Jesus Angulo[b], Hanne Peters[b], Thomas Peters[b], Dieter Blaas[a,*]

[a]*Max F. Perutz Laboratories, University Departments at the Vienna Biocenter, Department of Medical Biochemistry, Medical University of Vienna, Dr. Bohr Gasse 9/3, A-1030 Vienna, Austria*
[b]*Institute for Chemistry, University of Lübeck, Germany*

Received 10 February 2005; returned to author for revision 22 April 2005; accepted 13 May 2005
Available online 13 June 2005

Abstract

Concatemers of various numbers of the third ligand binding repeat of human very-low density lipoprotein receptor arranged in tandem were fused to maltose-binding protein and expressed as soluble polypeptides. These artificial receptors protected HeLa cells against infection with human rhinovirus serotype 2 (HRV2) to a degree that strongly increased with the number of repeats present; maximal protection was seen for the pentameric concatemer (MBP-V33333). This V3 pentamer neutralized HRV2 more efficiently than a recombinant protein with the entire ligand binding domain of the native receptor encompassing all 8 non-identical repeats. A concatemer of seven V3 modules (MBP-V3333333) was also less neutralizing. Neutralization was correlated with the degree of inhibition of virus binding to the cell surface. The results were in agreement with kinetic measurements using Biacore instrumentation demonstrating an increase in avidity with the number of modules present. At low concentrations of the receptor fragments, a 1:1 Langmuir kinetics was observed which became of complex type in the higher concentration range. This is most likely a consequence of receptor molecules simultaneously binding via several modules. Since there is no viral aggregation, neutralization of viral infectivity results from blockage of the receptor binding sites and possibly from inhibition of viral uncoating by crosslinking the viral capsid subunits via multi-module binding. Finally, the low affinity of the single V3 module allowed demonstrating the possibility of mapping the binding epitope of the V3 receptor fragment by saturation transfer difference nuclear magnetic resonance methodology.

Keywords: Concatemer; HeLa cell; Neutralization

Introduction

Human rhinoviruses (HRVs) are responsible for about 50% of all mild respiratory infections, essentially manifesting by a running nose (Couch, 1996). They are small positive sense single-stranded RNA viruses sharing the icosahedral capsid architecture and overall genome organization with other picornaviruses such as the polio- and coxsackieviruses, serious human pathogens. The RNA genome is roughly 7100 nucleotides in length and encodes a polyprotein that is co-translationally and autocatalytically processed into the four capsid proteins VP1, VP2, VP3, and VP4, and several non-structural proteins taking part in replication (for review on picornaviruses see (Semler and Wimmer, 2002)). For cell entry, 87 HRV serotypes use intercellular adhesion molecule 1 (ICAM-1), and 12 serotypes use members of the low density lipoprotein receptor (LDLR) family (Ledford et al., 2004; Vlasak et

* Corresponding author. Fax: +43 1 4277 9616.
E-mail address: dieter.blaas@meduniwien.ac.at (D. Blaas).
[1] Current address: Biomin Gesunde Tierernährung International GmbH, 3130 Herzogenburg, Austria.
[2] Current address: Zentrum für Anatomie und Zellbiologie, Medical University Vienna, Austria.

0042-6822/$ - see front matter © 2005 Elsevier Inc. All rights reserved.
doi:10.1016/j.virol.2005.05.016

al., 2005). Based on the amino acid sequences of VP1 and the available three-dimensional structures of the capsid proteins only, the principle underlying the distinction between the receptors could not be elucidated.

The ligand binding domain at the N-terminus of LDL-receptors is made up of several imperfect direct repeats, each about 40 amino acid residues in length. Each of the modules is stabilized by a Ca^{++} ion and three disulfide bonds. The low-density lipoprotein receptor (LDLR), the very-low density lipoprotein receptor (VLDLR), and the LDLR-related protein (LRP) contain 7, 8, and 31 such repeats (for review see (Strickland et al., 1995)). The ligand binding region is succeeded by a domain with similarity to the epidermal growth factor precursor interspaced with YWTD repeats. At least in LDLR, this part of the molecule adopts the conformation of a ß-propeller. At low pH, as it prevails in endosomes, the ligand binding domain folds back and interacts with this ß-propeller whereby bound ligands are out-competed (Rudenko et al., 2002). Proximal to the membrane is a more or less O-glycosylated region that is followed by the transmembrane domain and a cytoplasmic tail with NPXY motives responsible for clathrin-dependent internalization (Snyers et al., 2003).

Receptor derivatives have been envisaged as antivirals acting via competition for cellular binding sites; e.g., soluble ICAM-1 and bi- or penta-dentate ICAM-1-IgG, IgA, and IgM-fusion proteins have been shown to efficiently inhibit major group rhinovirus infection in vitro (Crump et al., 1993; Marlin et al., 1990; Martin et al., 1993; Ohlin et al., 1994) and in vivo (Shigeta, 1998). In the case of ICAM-1, this inhibition is not only due to competition with the cellular receptor but also to a catalytic, virus-neutralizing function; binding to the viral canyon, a cleft encircling the five-fold axes of icosahedral symmetry, promotes structural modifications resulting in RNA release (Nurani et al., 2003). Pursuing similar lines of research on minor group viruses, we have shown previously that preincubation of HRV2 with a selection of recombinant soluble LDLR or VLDLR derivatives also protects HeLa cells against infection (Marlovits et al., 1998a, 1998b, 1998c; Ronacher et al., 2000; Verdaguer et al., 2004). However, in contrast to ICAM-1, where only the tip of the N-terminal domain interacts with the virus, we recently presented evidence that repeat 5 together with repeat 1 and/or 2 of LDLR play a role in binding HRV1A. This suggests the possibility of multi-module attachment (Herdy et al., 2004).

Reconstruction of cryo-electron microscopy (cryo-EM) images from complexes between virus and a VLDLR fragment containing repeats 1 to 3 only (V123) allowed mapping of the binding site to the BC and HI surface loops of the capsid protein VP1 (Hewat et al., 2000). In a follow up study, a number of recombinant proteins with different combinations of the ligand binding repeats were used for complex formation and structure analysis by cryo-EM suggested that two consecutive modules were simultaneously bound to two non-identical sites on the symmetry related subunits of the viral capsid. Conversely, in the case of minireceptors composed of two repeats (e.g., the maltose-binding protein fusions of V23 and V33, i.e., MBP-V23 and MBP-V33), only a single repeat was found to contact the viral surface whereas the other one was disordered. This might be caused by the MBP presumably hindering attachment of the neighboring repeat (Neumann et al., 2003). However, there was no evidence for multivalent binding to identical sites and all available structural data suggested that VLDLR fragments with more than two modules attached via repeat 3 (with a possible minor contribution of repeat 2) but with no participation of the other repeats. During these studies, we observed substantial differences between the various receptor fragments with respect to their cell-protecting, virus neutralizing capacity. As our experiments also revealed that single repeats were virtually not neutralizing, we wondered whether artificial combinations of the modules would possibly attach in an ordered, multivalent fashion and thereby bind the virus with higher avidity. Therefore, we expressed various concatemers of V3 and assessed their attachment to HRV2 and their capacity to inhibit viral infection. We here show that the neutralizing activity is greatly enhanced upon concatenation. The activity was maximal for MBP-V33333 but decreased upon concatenation of seven copies of V3. The results suggest that MBP-V33333 adopts a conformation particularly favorable for attachment to the virus and thereby to prevent its binding to the cellular receptors.

Results

HRV2 binds membrane-immobilized receptor fragments in virus overlay blots

Concatemers of repeat 3 were expressed in bacteria as fusion proteins with MBP, refolded, purified, and similar amounts of the proteins were run under non-reducing conditions on a SDS-polyacrylamide gel. Proteins were electrotransferred to a PVDF membrane, and after blocking, receptors were revealed by using antibodies against LDLR. As seen in Fig. 1, upper panel, the receptor fragments were present at similar amounts and migrated in the gel as monomers; only in case of MBP-V33 a doublet and in case of MBP-V333 two weak bands of higher molecular mass were seen. They might represent products of aberrant folding or dimerization. As the higher M_r material also yielded bands with radiolabeled virus, the binding activity was not grossly impaired by these modifications. In the case of MBP-V333, the interaction with the virus appears even somewhat increased upon aggregation (compare amounts of monomer and presumed dimer of MBP-V333 with their virus binding activity, top and bottom panel in Fig. 1). MBP, used as a negative control, did not react with the antibodies.

Receptor associated protein (RAP) a specific chaperone, binds strongly to VLDLR and LRP and has been frequently used as an inhibitor of ligand binding (Bu et al., 1995). For

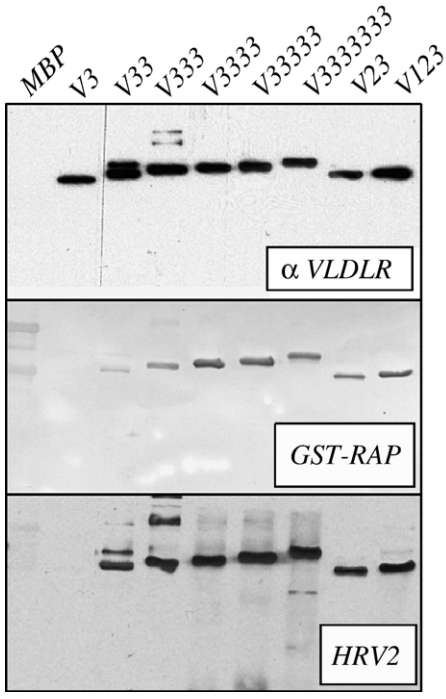

Fig. 1. Concatemers of repeat 3 of VLDLR bind HRV2. The concatemers indicated ("MBP" is omitted for simplicity) were run on a SDS 10% polyacrylamide gel under non-reducing conditions and transferred to a PDVF membrane. After blocking, the membrane was incubated with anti-VLDLR IgY (upper panel), with biotin-conjugated GST-RAP (middle panel), and with 30,000 cpm of [^{35}S]-methionine labeled HRV2 (lower panel). Detection was with HRP-conjugated anti-chicken IgY or with HRP-conjugated streptavidin followed by substrate, and by exposure to X-ray film, respectively.

control purposes and to ascertain that the receptors were correctly folded, a glutathione-S-transferase-RAP fusion protein (GST-RAP) was used to assess binding (Fig. 1, middle panel). In accordance with earlier data (Mikhailenko et al., 1999), GST-RAP failed to bind to the single repeat (MBP-V3) whereas it bound to all other fragments, although weakly to MBP-V33. MBP, cleaved from the fusion protein MBP-V33333 with factor Xa and collected in the flow through of a Ni-NTA column that retains the hexa-his tagged receptor-moiety, was used as control and showed only some very faint bands. These most probably originated from incompletely cleaved and partially degraded MBP-V33333 that had lost the hexa-his tag and was thus present in the sample at low amounts (Ronacher et al., 2000).

Virus binding activity was then assessed by incubation with [^{35}S]-labeled HRV2 followed by autoradiography. As seen in Fig. 1, lower panel, all concatemers of V3 bound HRV2; virus binding was comparable to that of receptors with the natural sequence of the repeats (compare MBP-V33 to MBP-V23 and MBP-V333 to MBP-V123). Only for MBP-V3, no virus binding was seen in this assay although its amount was similar to that of the other receptors as judged from Coomassie brilliant blue staining (not shown) and immunoblotting with VLDLR specific antiserum (Fig. 1, upper panel). Note that the difference in migration of the proteins is small due to the contribution of only 6.9 kDa of a single V3 module to the M_r of MBP (42.3 kDa).

V3-concatemers protect HeLa cells against infection by HRV2

The capacity of various VLDLR receptor constructs to neutralize infection of HeLa cells by HRV2 was then assessed. Two-fold serial dilutions of the purified concatemers were incubated for 30 min at room temperature with 100 $TCID_{50}$ of HRV2. The mixtures were then transferred onto monolayers of HeLa cells grown in 96-well plates and the infection was allowed to proceed for 3 days. In this assay, the absence of cell lysis (as detected by crystal violet staining of intact cells) indicates complete neutralization of the virus by the soluble receptors. Partial neutralization also leads to complete lysis of the culture because even few newly produced virions spread and infect other cells during incubation for 3 days. Soluble "natural" VLDLR minireceptors encompassing repeats 1 to 3 (MBP-V123) and 1 to 8 (MBP-V12345678) were included for comparison. Fig. 2 illustrates that MBP-V33333 protects HeLa cells most efficiently against viral infection. On a molar basis, it was about 250 (2^8) times more efficient (i.e., 250 times less MBP-V33333 was required for neutralization) than MBP-V123 in this assay. On the other hand, the neutralization efficiency of MBP-V33 was much lower than that of MBP-V123 and just concentrations exceeding 32 nmol/l led to cell protection (data not shown but see also (Verdaguer et al., 2004)). This might indicate that the first repeat after the MBP contributes much less to binding, presumably because of steric problems caused by the MBP (Neumann et al., 2003; Ronacher et al., 2000; Verdaguer et al., 2004). The fragment containing three repeats, MBP-V333, was only slightly more neutralizing than MBP-V123 and slightly less than MBP-V1–8. However, virus neutralization by MBP-V3333 and MBP-V33333 was at least 20 times higher as compared to the entire native ligand binding domain. MBP-V3333333,

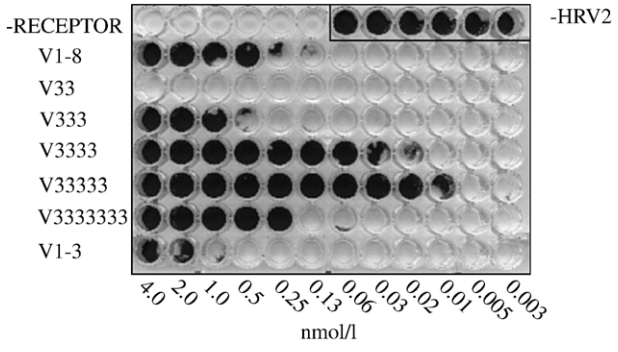

Fig. 2. MBP-fusions with concatemers of repeat 3 of VLDLR protect HeLa cells against infection with HRV2. Serial two-fold dilutions of the receptor constructs were incubated with 100 $TCID_{50}$ of HRV2 for 60 min at room temperature and the mixture was applied onto HeLa cell monolayers grown in microtiter wells. After incubation at 34 °C for 3 days, cells remaining attached to the plastic were stained with crystal violet.

the largest fragment tested, neutralized similarly to MBP-V12345678; this might be taken to indicate that this receptor is too big to allow for an ordered attachment; possibly, it prevents other soluble receptors from binding but also leaves some sites accessible for cell surface attachment. Cryo-EM of complexes between this receptor and HRV2 showed no evidence for aggregation (Neumann et al., 2003). This indicates that the additional repeats are not available for binding another virus particle and that neutralization is most probably based on blockage of the binding sites.

Soluble receptors reduce the number of cells becoming infected upon viral challenge

To examine more accurately the concentration dependence of the neutralization of HRV2 by the various VLDLR fragments, we counted the number of virus-producing cells in the presence of the soluble mini-receptors 1 day after infection. For this experiment, M4-LDLR cells were used. This is a murine LDLR−/− and LRP−/− cell line that has been stably transfected to express human LDLR (Reithmayer et al., 2002). These cells were selected because they have the capacity, although limited, to replicate a mouse adapted HRV2 ($HRV2_L$; (Yin and Lomax, 1983)) but are not readily lysed by the virus. This allows for monitoring the infection by counting the number of cells actively replicating the virus after staining for virus-specific proteins.

M4-LDLR cells were seeded on coverslips and infected with $HRV2_L$ at an MOI of 10. The MOI was chosen such as to allow for counting virus-producing cells under the microscope 1 day after infection by using immunofluorescence microscopy detection with the monoclonal anti-HRV2 antibody 8F5 (Skern et al., 1987) followed by FITC-conjugated anti-mouse antibody. The virus was pre-incubated with increasing concentrations of the MBP-VLDLR fragments prior to challenging the cells. As control, virus was incubated without receptor. Only MBP-V33333 and MBP-V123, exhibiting a strong difference in the neutralization capacity (see Fig. 2), were used in this experiment. Fig. 3A shows the ratio between the number of cells infected in the presence of the soluble receptors and the number of cells infected in their absence. For MBP-V123-mediated neutralization of $HRV2_L$, the number of infected cells decreased gradually upon increasing the concentration of receptor. However, the curve only asymptotically approached zero infected cells suggesting that receptor concentrations largely exceeding 30 nmol/l would be needed to fully protect the cells (i.e., that none of the cells becomes infected). In contrast, complete neutralization was readily achieved by MBP-V33333. Not a single infected cell was seen at 7 nmol/l of MBP-V33333, whereas in the presence of MBP-V123 at 30 nmol/l (and even at 60 nmol/l; not shown) some few cells clearly showed viral protein synthesis. These results are consistent with the neutralization data shown in Fig. 2, where, on a molar basis, ~250 times (2^8) more MBP-V123 than MBP-V33333 was needed to fully protect the cells.

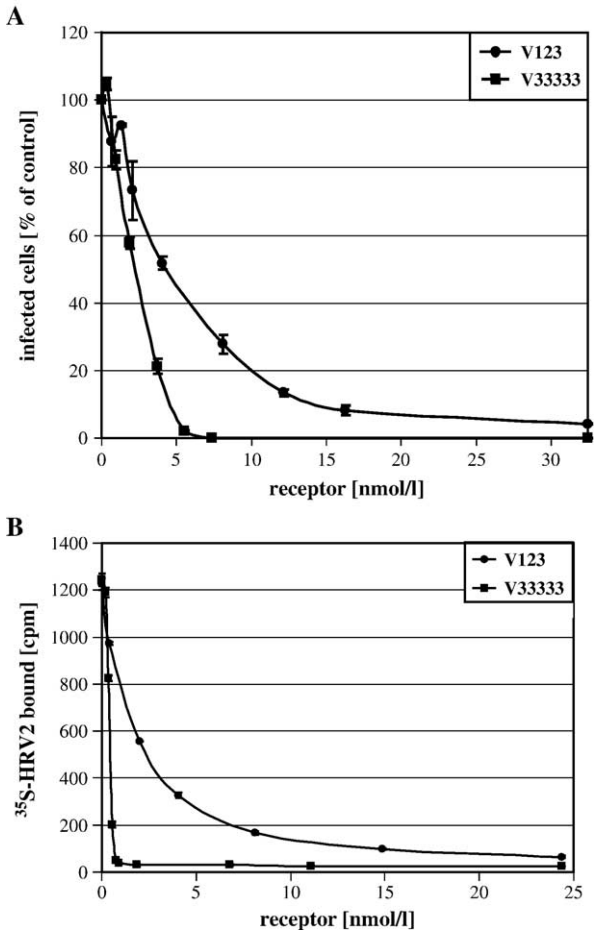

Fig. 3. Concatemers of V3 protect a mouse fibroblast cell line expressing human LDLR against HRV2 infection by inhibition of virus binding. (A) $HRV2_L$ was preincubated with the concentrations of MBP-V123 or MBP-V33333 indicated for 1 h at room temperature and transferred onto M4-LDLR cells grown on coverslips. Cells were washed and further incubated in infection medium. The next day, virus-infected cells were identified upon staining viral antigens with mAb 8F5 and secondary FITC-conjugated antibody. Cells producing viral antigen were counted under the fluorescence microscope as described in Materials and methods. The number of cells infected in the presence of the receptors is presented as percentage of the number of cells infected in the absence of receptor. Each point corresponds to the mean of two independent experiments with indicated span. (B) Radiolabeled HRV2 (~10,000 cpm) was preincubated with the receptors for 30 min at room temperature and the mixture was transferred onto subconfluent M4-LDLR806 cells grown in 24-well plates. After 30 min at room temperature, the cells were washed 3 times and cell associated radioactivity was determined by liquid scintillation counting. Each point represents the mean of duplicate measurements with indicated span.

Virus binding is inhibited by recombinant receptor fragments

Viral infectivity can be inhibited by agents (i) competing with the cellular receptor for viral binding sites, (ii) by prevention of uncoating (i.e., RNA release), (iii) by inactivation of the virus (e.g., as occurs upon binding of ICAM-1 to some major group HRVs; this receptor binds into the viral canyon and is believed to push apart the subunits like a wedge or to hold them in a more open

conformation thereby promoting structural changes ultimately leading to uncoating (Xing et al., 2003), or (iv) by aggregation. Having ruled out the latter two possibilities (see above and (Hofer et al., 1994)), we wondered to what extent cell binding of radioactively labeled HRV2 was inhibited by the VLDLR fragments. For this experiment, M4-LDLR806 cells were employed. These cells stably express a truncated version of human LDLR lacking 33 amino acid residues in the cytoplasmic domain including the coated pit localization signal. They express high amounts of LDLR on the plasma membrane and therefore have a high virus-binding capacity (Reithmayer et al., 2002; Snyers et al., 2003). Metabolically labeled [^{35}S]-HRV2 was incubated with increasing concentrations of MBP-V123 or of MBP-V33333 for 30 min at room temperature. The mixtures were then transferred onto the cells and the incubation was continued for 30 min. After washing three times, the cells were lysed and cell-associated radioactivity was determined by scintillation counting. Like for the neutralization of infectivity, virus binding (and internalization that also occurs under these conditions) was found to be prevented by much lower concentrations of MBP-V33333 as compared to MBP-V123 (Fig. 3B). Similarly to the lack of a complete block of infection (Fig. 3A), even at the highest concentration, MBP-V123 did not completely abrogate virus binding, whereas very low concentrations of MBP-V33333 completely prevented attachment of the virus. The difference between the two fragments with respect to their capacity to block virus binding was even more accentuated than in the neutralization assay (Fig. 3A). Curve fitting to the hyperbolic function $B = B_{\max} - \frac{(B_{\max} - B_{\min})[R]^{\mathrm{Hill}}}{K_{\mathrm{D}}^{\mathrm{Hill}} + [R]^{\mathrm{Hill}}}$ where B is bound receptor, R is receptor concentration, and Hill is the Hill coefficient yielded a K_{D} of 1.6 nmol/l for MBP-V123 and a K_{D} of 0.4 nmol/l for MBP-V33333 clearly indicating stronger binding of the latter concatemer. Interestingly, the Hill coefficient was about 1 for MBP-V123 and about 6 for MBP-V33333. This might be due to strong cooperativity of the modules in the pentamer suggesting that binding of one repeat facilitates binding of the others. Taken together, these results suggest that neutralization of HRV2-infection by the VLDLR-derived fragments is, at least to a large part, due to inhibition of binding of the virus to the cellular receptors. They further suggest that MBP-V33333 readily covers all receptor binding sites, whereas binding of MBP-V123 even at the highest concentration tested leaves some sites on the viral surface available for binding of cell surface receptors. However, the observed effect might also only be due to the considerable differences in affinity/avidity and the strong cooperativity observed for MBP-V33333.

Kinetic parameters of the HRV2-receptor interaction

In order to assess whether the inhibitory activity of the receptor derivates was correlated with their affinity/avidity for the virus, the kinetic parameters of the binding reaction were determined using a Biacore apparatus. Determination of the binding kinetics requires the virus to be immobilized on the sensor chip. The receptor is then injected in a constant flow over this modified surface. Binding leads to an increase of the mass at the surface of the chip which is translated into a signal expressed as resonance units (RU). Dissociation of the bound receptor occurs as soon as plain buffer solution is being passed over the surface. After each association–dissociation cycle, any residual receptor has to be completely detached for the signal to return to the baseline. This is usually brought about by flushing with low pH buffer and complete detachment of the receptors in Biacore experiments with HRV3 and with ECHO11, other picornaviruses, was achieved in this way (Casasnovas and Springer, 1995; Lea et al., 1998). However, in our case, using the same conditions, the receptor was not removed and pH values below 5.6 denatured HRV2, preventing re-use of the chip ((Gruenberger et al., 1991) and data not shown). Therefore, we chose to use a sandwich type of assembly by covalently immobilizing MBP-V33333 at high density followed by attachment of HRV2. A similar sandwich method has been used previously for the determination of the parameters underlying antibody binding to Semliki forest virus (Hammar et al., 2003). Initial experiments showed that virus became tightly bound to the surface carrying MBP-V33333 and was not dissociated even upon washing with buffer for several hours (not shown). Most probably, this is not only due to high avidity (functional affinity) of MBP-V33333 for the virus but also to attachment of the virion via several receptor molecules. For regeneration, virus, together with any residual receptor remaining after the dissociation phase, was detached with low pH buffer and new virus was bound to the chip-immobilized receptor for the next association–dissociation cycle. The sandwich also exploits the high specificity of the receptor to only bind native virus and no subviral particles. Such particles might be present in the preparation since they are intermediates of the uncoating process. “A-particles” have lost the innermost capsid protein VP4, whereas “B-particles” have additionally lost the genomic RNA (Lonberg Holm and Noble Harvey, 1973).

In a first set of experiments solutions of MBP-V123 at concentrations between 4 nM and 200 nM were added to the flow over HRV2 immobilized to the chip-bound MBP-V33333. The tracings showed typical association–dissociation curves (Fig. 4A, gray traces). However, attempts to determine the kinetic parameters of the reaction with the BiaEvaluation software using the “global fit” procedure that simultaneously fits association and dissociation rate constants, k_{on} and k_{off}, at varying receptor concentrations revealed that neither of the available models was able to fit the curves satisfactorily. For example, the simple 1:1 Langmuir model yielded a very poor fit, and meaningful kinetic parameters could not be derived (see dashed lines in Fig. 4A). All attempts to arrive at acceptable fits by using more complex binding models also failed (data not shown). Therefore, we tried to analyze the data by individually fitting

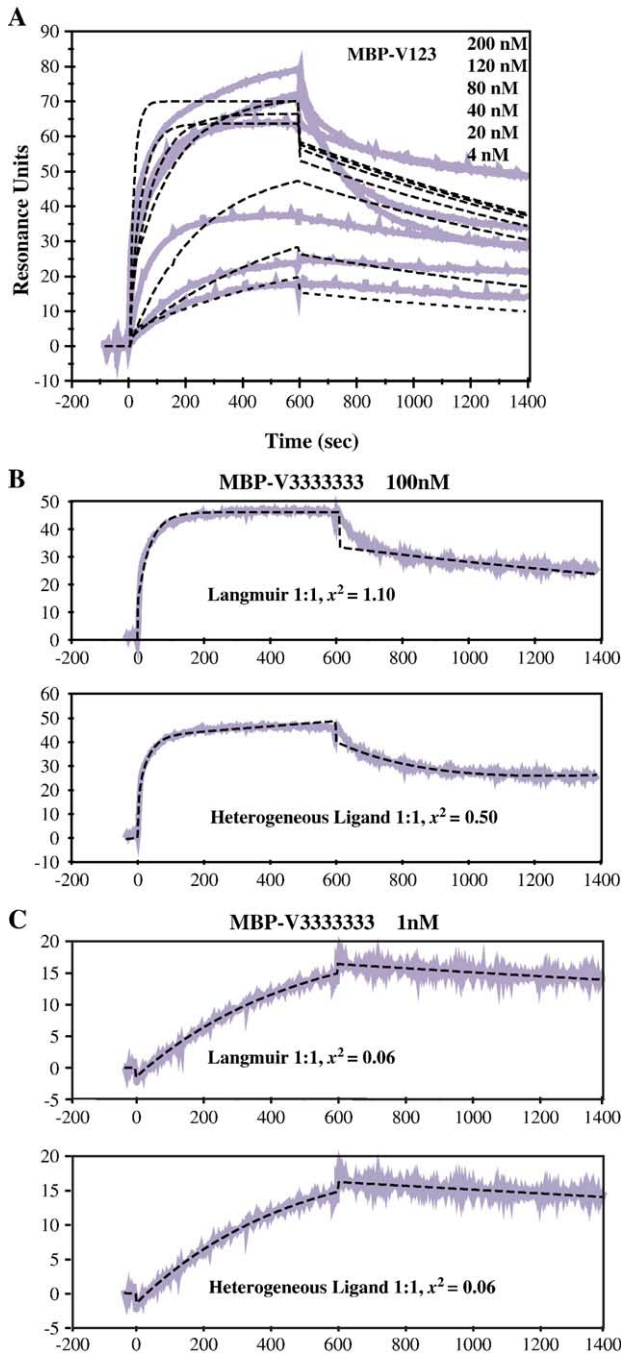

Fig. 4. Kinetics of receptor binding to HRV2 as determined by surface plasmon resonance. HRV2 was attached non-covalently to MBP-V33333 immobilized to F1 chips. (A) MBP-V123 was then added to the flow at the concentrations shown to monitor the binding phase. Then, only buffer was run over the chip to monitor the dissociation phase. After each measurement, the surface was regenerated by removing residual bound receptor together with the virus by rinsing with low pH buffer and new virus was bound to the immobilized receptor. Data were only included in the analysis when the amount of attached virus was similar. The final data set was subjected to the "Global Fit" procedure using the 1:1 Langmuir model and the "Heterogenous Ligand" model as provided in the BiaEvaluation software. (B and C) Langmuir 1:1 fit of the binding and dissociation of MBP-V3333333 at 100 nM (B) and at 1 nM (C) demonstrating the good fit in the low but the bad fit in the high concentration range. Measured data, thick grey lines; fit data, dashed black lines.

the binding curves employing "simultaneous fit" of k_{on} and k_{off}. This revealed interesting differences between curves at high and low receptor concentrations (exemplified for MBP-V3333333 in Figs. 4B and C). For higher concentrations, the fits were poor. However, when the lowest concentrations were utilized the simple (1:1) binding model yielded almost excellent fits (compare Figs. 4B and C; 100 nM and 1 nM receptor concentration). The quality of the fit is also reflected in high and low χ^2 values, respectively. A slight improvement at the higher concentrations was seen when invoking a more complex binding model such as the heterogeneous ligand model that, in this particular case, assumes the presence of two different binding sites on the immobilized virus (top and bottom panels in Fig. 4B). On the other hand, at 1 nM receptor concentration the fit was not improved any further by applying a two-site heterogeneous ligand binding model (top and bottom panels in Fig. 4C). Similar results were obtained for the other concatemers (not shown). For these reasons, only the binding curves at the lowest concentrations were analyzed using a simple Langmuir (1:1) binding model except for MBP-V123, where the "two site heterogeneous ligand model" gave a better fit. The χ^2 values were generally below 0.1. Table 1 shows that the measured affinity of the various receptor concatemers increases with the number of V3 copies present until MBP-V33333, where the affinity is apparently too high to be measurable by this method. In accordance with the neutralization data, it does not further increase upon addition of two more V3 repeats but rather decreases. Receptors with the natural sequence of modules (i.e., MBP-V12345678 and MBP-V123) display intermediate and low affinities, respectively, as compared to the concatemers of module 3.

STD NMR experiments to study the binding of receptor fragments

Over the past few years, the STD NMR technique (Mayer and Meyer, 2001) has become very popular (for a review, see (Meyer and Peters, 2003)). The technique allows to rapidly identify binding ligands from mixtures, and, more importantly, yields structural information on ligand binding epitopes at atomic resolution (Mayer and Meyer, 2001). Recently, we have shown that it is possible to detect and characterize the binding of small organic molecules to the hydrophobic pocket of the virus (Benie et al., 2003). Therefore, we wondered whether this technique would be applicable to study the binding of VLDLR receptor fragments to HRV2. The STD NMR technique requires one binding partner to be small as compared to the other, a condition which is met by the receptor (7 kDa per module) and the virus (8 MDa). The kinetics of the interaction between the larger concatemers and the virus, as determined by surface plasmon resonance (see Table 1), is far too slow for STD NMR experiments. Therefore, we chose the single repeat V3 for initial NMR experiments. MBP was removed from the MBP-V3 by cleavage with factor Xa (Ronacher et

Table 1
Kinetic and equilibrium binding constants for various MBP-VLDLR receptor derivatives as determined with the Biacore instrument using the "simultaneous fit" method

Analyte (MBP-)	k_{on} (M^{-1} s^{-1})	k_{off} (s^{-1})	K_D (mol/l)	c (nmol/l)	Model
V33333	n.a.	n.a.	$<10^{-12}$	1	Langmuir
V3333	2.0×10^{6}	3.2×10^{-5}	1.6×10^{-11}	1	Langmuir
V3333333	3.7×10^{6}	1.1×10^{-4}	3.0×10^{-11}	1	Langmuir
V12345678	1.5×10^{6}	1.8×10^{-4}	1.2×10^{-10}	3	Langmuir
V333	9.2×10^{5}	3.4×10^{-4}	3.7×10^{-10}	5	Langmuir
V123	8.4×10^{6}	2.2×10^{-2}	1.4×10^{-8}	2	Heterogeneous ligand
V3	2.2×10^{6}	5×10^{-1}	4.5×10^{-7}	10,000	Langmuir

Data were derived from experiments with the receptors present at concentration c. Receptor fragments are arranged in the order of decreasing functional affinity (top to bottom). n.a. not applicable; data could not be derived because the affinity was beyond the measuring limits of the instrument.

al., 2000) and V3 was purified via affinity chromatography on a Ni-NTA column making use of the appended His6-tag.

A STD NMR spectrum obtained for V3 in the presence of native virus is shown in Fig. 5, demonstrating strong STD signals. Control experiments (see Materials and Methods) showed that no direct irradiation of V3 occurred under the chosen experimental conditions. It is noteworthy that an on-resonance frequency of −4 ppm still yielded a significant saturation of the virus ^{1}H NMR resonances. Although a complete chemical shift assignment is not yet available, it is clear that the STD NMR spectrum contains the information required to determine the binding epitope. Fig. 5 demonstrates that different resonances of V3 receive different amounts of saturation. These differences will be translated into a binding epitope as soon as an assignment of V3 is available. In the present analysis, different spectral regions of the STD spectrum were integrated (values not shown) which enabled us to classify signals that receive high or low amounts of saturation (up- and down-triangles, in Fig. 5). The better resolution in the region of backbone amide and aromatic protons (between 6.5 and 10 ppm) highlights these differences (Fig. 5).

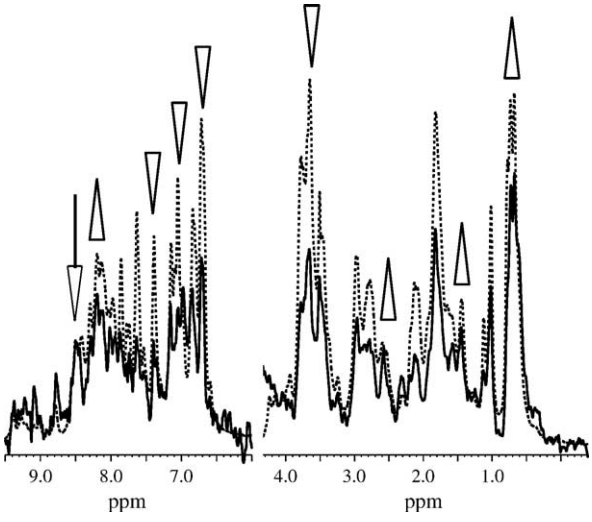

Fig. 5. STD NMR spectrum of V3 in the presence of HRV2. Overlaid NMR spectra (500 MHz, 288K; dotted lines) 1D ^{1}H NMR reference spectrum of a mixture of HRV2 and a 500-fold excess (over binding sites) of V3, and 1D STD NMR spectrum of the same sample (plain lines). The intensities of the down-field spectral region (6–9.4 ppm) were expanded for better visualization. The arrow indicates the signal used to match the intensities of the reference and saturated spectrum. Up-triangles show some of the signals receiving a larger amount of saturation. Down-triangles indicate signals with low level of saturation in the difference spectrum. Distances between protons in V3 and in the binding site of HRV2 can be derived from the difference between the intensities of the STD NMR and the reference ^{1}H NMR signals.

Discussion

In this paper, we have quantified the contribution of single modules to virus neutralization and inhibition of virus binding by using artificial concatemers of V3, synthesized as recombinant fusion with maltose binding protein. In virus overlay blots, all the concatemers bound HRV2, whereas no interaction of the single module MBP-V3 with the virus was detected under these particular conditions. In this respect, HRV2 resembles RAP that also requires more than one repeat for binding to LRP, which is believed to harbor at least two independent RAP binding sites (Mikhailenko et al., 1999). It should be mentioned that some weak binding of MBP-V3 to HRV2 can be detected at very high concentrations in overlay blots (Nizet et al., submitted for publication) and that MBP-V3 displays marginal virus inhibition (Verdaguer et al., 2004). The virus overlay blots failed to reveal large differences in virus binding of the different concatemers presumably because the receptors were present at high concentration within the bands. In contrast, in cell protection assays, a clear difference was seen in serial two-fold dilutions of the receptor. Interestingly, MBP-V33333 had the strongest cell protection capacity. It would be interesting to know how many receptor molecules must bind per virion to achieve neutralization. However, due to the high and ill-defined ratio between the total number of viral particles and infectious viral particles of between 24:1 and 240:1 (Abraham and Colonno, 1984), this value is extremely difficult to determine.

Results of earlier experiments with complexes between MBP-V33333 and HRV2 suggested simultaneous binding of multiple VLDLR ligand binding repeats to the viral surface. Virions carrying between 0 and 12 receptor

molecules could be separated by capillary electrophoresis (Konecsni et al., 2004); in combination with the cryo-EM (Neumann et al., 2003) and X-ray data (Verdaguer et al., 2004), this suggested already that the receptor molecules must have attached around the five vertices of the icosahedron. Our present results are in complete agreement with this model. The longer receptor MBP-V333333 or MBP-V12345678 were less neutralizing because they might fail to attach in an ordered fashion.

The weakly neutralizing MBP-V123 and the strongly neutralizing MBP-V33333 were examined with respect to inhibition of virus binding to M4-LDLR806 cells and to neutralization of viral infection by observing de novo viral protein synthesis on the single cell level. It turned out that MBP-V123 did neither inhibit virus binding nor cell infection completely even at the highest concentrations tested. Conversely, MBP-V33333 was extremely effective in both respects. This might be interpreted as an incomplete coverage of receptor binding sites by MBP-V123. Since V1 fails to bind all together (Neumann et al., 2003) and only V2 and V3 can bind, one can envisage a situation in which two copies of MBP-V123 cover four binding sites but leave one open for attachment to a receptor on the cell membrane. In the case of MBP-V33333, all potential sites might be rendered inaccessible, which is reflected in the virtual absence of cell binding and infection already at low concentrations.

Kinetic measurements with Biacore instrumentation point into the same direction and show that the functional affinity between the various receptors is quite different. However, whereas similar experiments with HRV3 and soluble ICAM-1 (Casasnovas and Springer, 1995) and with ECHO11 and soluble DAF (Lea et al., 1998) gave textbook like binding and dissociation curves, the interaction between HRV2 and the various soluble receptors was complex and the curves followed simple kinetic models only at low concentrations. Nevertheless, using only single curve fitting, kinetic constants, and equilibrium dissociation constants could be derived (Table 1). Whereas the strongest neutralizer MBP-V33333 exhibited an affinity beyond the upper measuring range of the instrument, all other receptors bound with lower affinity and their binding parameters could be determined. Only in case of MBP-V3 micromolar concentrations were required to obtain an interpretable signal. Taken together, this suggests that the geometry of MBP-V33333 is such as to fit extremely well onto the vertex of the virion and does not leave any binding site free. The values of the dissociation constants were in the range of 10^{-11} Mol/l (for MBP-V3333) and 10^{-7} Mol/l for (MBP-V3). The complex kinetics at higher concentrations is most probably due to simultaneous attachment of more than one copy of the larger receptors to the five attachment sites at the five-fold axis involving different numbers of modules. The association rate constants were similar for all receptor constructs and were in the order of 10^6 Mol^{-1} s^{-1} (Table 1). Association is thus much faster than in the case of ICAM-1 binding HRV3 (biphasic with 2450 and 135 Mol^{-1} s^{-1} (Casasnovas and Springer, 1995)) and still faster than for decay accelerating factor (DAF) binding Echovirus 11, another picornavirus (150,000 Mol^{-1} s^{-1} (Lea et al., 1998)). This probably reflects the different exposure of the binding sites; ICAM-1 binds inside the canyon, and DAF most probably binds ECHO 12 at the two-fold axis in one or the other orientation that have been determined for ECHO 7 (He et al., 2002) and ECHO 11 (Bhella et al., 2004)), respectively. Conversely, VLDR binds to the extremely exposed star-like mesa. Furthermore, once the first module has bound, the others certainly bind very quickly to the neighboring sites. The dissociation rate constants were between 3.2×10^{-5} (for MBP-V3333) and 1×10^{-1} (for MBP-V3), which indicates that dissociation occurs more slowly the more binding repeats are present. This resembles very much the situation of the bivalent IgG molecules; if one of the two arms dissociates, it nevertheless remains in the vicinity and re-binding is strongly favored as compared to a monovalent Fab fragment (Hewat and Blaas, 2001).

The kinetic on- and off-rates of V3 lay within the range suitable for epitope mapping via STD NMR. We thus assessed the possibility to investigate the binding of the VLDLR receptor to HRV2 and to determine its binding epitopes via this technique. The pilot experiments described here unambiguously demonstrate that it is indeed possible to obtain high quality STD NMR spectra that contain all the information required to define the binding epitope on the receptor (Fig. 5). The assignment of the ^{1}H NMR spectrum of V3 is underway and a more detailed NMR analysis will be published elsewhere. This is the first time that STD NMR experiments were applied to a system consisting of a native virus and a receptor fragment of M_r 7.3 kDa. This is remarkable as STD NMR is usually employed for the characterization of the binding of small ligands, i.e., with a molecular weight below 2 kDa, to large receptor proteins. Thus, this is a key experiment paving the way for the rapid characterization of the interaction between a multitude of receptor modules and various HRV serotypes at atomic resolution.

The multi-module attachment identified here accounts for the considerable increase in neutralization potency and binding strength of receptor concatemers with the number of modules present. It also tentatively explains how the different minor group HRV serotypes bind to their host cells; the various modules present in the natural receptors might exhibit different affinities versus the twelve serotypes which is compensated by the simultaneous attachment via several modules as exemplified by HRV1A binding very weakly to human LDLR but strongly to human LRP (Herdy et al., 2004).

Antibodies and receptors may have overlapping but not identical binding sites. The multitude of slightly different receptor modules (7 in LDLR, 8 in VLDLR, and 31 in LRP) presumably cope more easily with changes at the virus surface occurring upon escape from neutralizing antibodies in that reduction of binding affinity for one given module

might be compensated by the increase of affinity for another module.

Materials and methods

Construction, expression, and purification of the V3 concatemers

The construction of MBP-V123 (maltose binding protein fused to repeats 1, 2, and 3 of the ligand-binding domain of human VLDLR) was described previously (Ronacher et al., 2000). MBP–concatemer fusions containing various numbers of repeat 3 (V3) were prepared essentially as described (Konecsni et al., 2004). Briefly, V3 was first amplified from a plasmid containing the entire sequence of human VLDLR (Marlovits et al., 1998b; Sakai et al., 1994) using primers 5′-ATGCGGATCCAACATGCCGCATACATG and 5′-GCAGCCCGGGACTCATATGGCACTGTTC and introduced into the vector pMalc2b using restriction sites *Bam*HI and *Xma*I. The resulting plasmid encodes V3 (amino acid residues 112 to 151 of the VLDLR precursor sequence (Swissprot entry P98155) fused at its N-terminus to MBP via a linker of 11 amino acid residues and at its C-terminus to a hexa-histidine tag. The plasmid was cleaved with *Sma*I to generate blunt ends immediately in 3′ of the V3 sequence. Another V3-coding sequence was made by PCR using primers 5′-GGGACATGCCGCATACATGAAATC and 5′-ATTGCCACAGTTTTCTTCATC and *Pfu* DNA polymerase. This fragment was ligated into the *Sma*I site. After transformation, colonies containing plasmid pMal with 1, 2, 3, or 4 copies of V3 fused to MBP were obtained. To generate longer concatemers, a plasmid containing MBP-V3333 was cut with *Sma*I and ligated with the same PCR fragment. This gave rise to additional concatemers with 5 and 7 copies of V3 fused to MBP. Expression, purification, and refolding were carried out essentially as described previously with the exception that the GST-RAP column material was not used to promote the folding reaction (Ronacher et al., 2000).

Ligand binding assay

Receptors were separated on a SDS 10% polyacrylamide gel under non-reducing conditions (Marlovits et al., 1998b) and electrotransferred to a PVDF membrane. The membrane was blocked with Tris-buffered saline (TBS) containing 2% non-fat dried milk and 2% bovine serum albumin (blocking buffer) for 1 h, and incubated with HRV2 metabolically labeled with [^{35}S]-methionine/cysteine (Neubauer et al., 1987) for 1 h at room temperature. The membrane was washed with blocking buffer, dried and exposed to X-ray film. Glutathione-S-transferase fused receptor associated protein (GST-RAP) was produced as described (Herz et al., 1991). For immunological detection, an IgY fraction prepared from eggs of a chicken immunized with recombinant human VLDLR was used.

Cell protection assay

HeLa-H1 cells (Flow Laboratories) were seeded in 96 well plates and grown to about 90% confluence in minimal essential medium (MEM) containing 10% fetal calf serum, 100 U/ml penicillin, 100 μg/ml streptomycin, and 2 mM L-glutamine. HRV2, at 100 $TCID_{50}$ (Blake and O'Connell, 1993), was incubated with serial two-fold dilutions of the receptor fragments in infection medium (as above but containing 2% fetal calf serum and 30 mM $MgCl_2$) for 30 min at room temperature prior to challenge of the cells. Upon incubation for 3 days at 34 °C, cells remaining attached to the plastic were stained with crystal violet (0.1% in water) and photographed. For the single cell protection assay, equal numbers of M4 cells, transfected to stably express human LDLR (M4-LDLR), were seeded on coverslips. They were infected at 34 °C for 20 min with $HRV2_L$ (MOI = 10) which had been pre-incubated for 1 h with increasing amounts of the soluble receptors. After washing away excess virus, cells were incubated in culture medium until the next day; virus producing cells were then detected by indirect immunofluorescence microscopy (Snyers et al., 2003) using the monoclonal antibody 8F5 directed against a sequential epitope on VP2 of HRV2 (Skern et al., 1987). Cells strongly stained in at least 25 different and randomly chosen fields were counted under the microscope for each receptor concentration, giving an average of successfully infected cells. This number was related to the number of cells producing virus in the absence of soluble receptor which was set to 100% (i.e., no neutralization). The experiment was performed two times.

Inhibition of binding of radioactively labeled HRV2

Equal numbers of M4 cells stably expressing a truncated version of human LDLR lacking the last 33 amino acid residues of the cytoplasmic tail including the clathrin localization signal (M4-LDLR806 cells) were seeded in 24-well plates. [^{35}S]-labeled HRV2 (~10,000 cpm) was mixed with increasing amounts of the soluble receptors, as in the cell protection assay, and incubated for 30 min at room temperature. The mixture was then transferred onto the cells and left for 30 min at room temperature. After washing three times with PBS, the cell-associated radioactivity was determined by liquid scintillation counting. Note that the amount of virus used in this experiment was almost the same as for the cell protection assay of M4-LDLR cells, as determined from the $TCID_{50}$ of the radioactive virus.

Kinetic measurements

Kinetic rate constants were determined on a Biacore 3000 instrument (Biacore International AB, Switzerland) using F1 chips manufactured by the same company following standard protocols for surface plasmon resonance

methodology (Lee et al., 2005). For assembly of the receptor-virus sandwich, MBP-V33333 at 150 μg/ml was immobilized on chips after activation with EDC/NHS in 20 mM Na-acetate buffer (pH 4) for 20 min and remaining active groups were deactivated with ethanolamine essentially following the standard protocol of the supplier. Next, purified HRV2 (~20 μg/ml) in 10 mM HEPES, 150 mM NaCl, 2 mM $CaCl_2$ (pH 7.4) was allowed to attach under a flow rate of 5 μl/min resulting in immobilization of 300 to 500 resonance units (RU). To maximize the reproducibility, care was taken to immobilize the same amount of virus for each series of experiments. In the reference cell MBP alone was immobilized on the chip using a pH of 4.5 during coupling. The surface was regenerated with system buffer of pH 2. This resulted in removal of eventually attached receptor together with the virus. Thus, new virus had to be bound prior to carrying out the next adsorption/desorption measurement cycle.

NMR experiments

Measurements were carried out on a Bruker DRX 500 spectrometer equipped with a 5-mm inverse triple-resonance probe head at 288 K. Samples were prepared in 500 μL 90% H_2O: 10% D_2O buffer containing 150 mM NaCl, 8 mM $CaCl_2$, and 25 mM TRIS buffer (pH 7.5). The concentration of the protein was 0.75 mM. Buffer was exchanged using a PD10 column (receptor), and by ultrafiltration with a Vivaspin (Vivascience) membrane with a cut-off value of 50 kDa (HRV2). Virus was mixed with the receptor to give a final concentration of ~23 nM (~500-fold excess of receptor over the binding sites). One-dimensional STD NMR experiments were recorded without spin-lock field because, due to the natural broadening of the resonances from the virus particles, no signals were observed. The suppression of the strong water signal was carried out using the WATERGATE sequence. Saturation was achieved by using a train of 40 selective Gaussian pulses with a duration of 49 ms and a spacing of 1 ms. The relaxation delay was 1.5 s. Irradiation was performed at −4 ppm for the on-resonance experiment, while for the off resonance spectrum, the frequency was set to 40 ppm. Subtraction of both spectra was performed internally via phase cycling. The experimental conditions were optimized by performing several 1D STD NMR control experiments with different on-resonance frequencies with the receptor sample in the absence of virus to verify that there was no effect on the receptor resonances for an on resonance frequency of −4 ppm. For the 1D NMR reference spectrum, 128 scans were recorded, and 8192 for the 1D STD NMR spectrum with 4 and 16 dummy scans, respectively.

Acknowledgments

We thank Irene Gösler for virus preparation and Peter Chiba for help with the fitting of the equilibrium binding data. This work was funded by the Austrian Science Foundation grant #P-16699 MOB. T.P. thanks the German Research Council (DFG) for a grant (Pe 494/4-2 and Me 1830/1-1). J.A. is a Marie-Curie fellow of the EU's Sixth Framework Programme (MEIF-CT-2003-500861).

References

Abraham, G., Colonno, R.J., 1984. Many rhinovirus serotypes share the same cellular receptor. J. Virol. 51, 340–345.

Benie, A.J., Moser, R., Bauml, E., Blaas, D., Peters, T., 2003. Virus–ligand interactions: identification and characterization of ligand binding by NMR spectroscopy. J. Am. Chem. Soc. 125, 14–15.

Bhella, D., Goodfellow, I.G., Roversi, P., Pettigrew, D., Chaudhry, Y., Evans, D.J., Lea, S.M., 2004. The structure of echovirus type 12 bound to a two-domain fragment of its cellular attachment protein decay-accelerating factor (CD 55). J. Biol. Chem. 279, 8325–8332.

Blake, K., O'Connell, S., 1993. Virus culture. In: Harper, D.R. (Ed.), Virology Labfax. Blackwell Scientific Publications, West Smithfield, London EC1A 7BE, UK, pp. 81–122.

Bu, G.J., Geuze, H.J., Strous, G.J., Schwartz, A.L., 1995. 39 kDa receptor-associated protein is an ER resident protein and molecular chaperone for LDL receptor-related protein. EMBO J. 14, 2269–2280.

Casasnovas, J.M., Springer, T.A., 1995. Kinetics and thermodynamics of virus binding to receptor—Studies with rhinovirus, intercellular adhesion molecule-1 (ICAM-1), and surface plasmon resonance. J. Biol. Chem. 270, 13216–13224.

Couch, R.B., 1996. Rhinoviruses. In: Fields, B.N., Knipe, D.M., Howley, P.M. (Eds.), Fields Virology, vol. 1. Lippincott-Raven Publishers, Philadelphia, pp. 713–734 (2 vols).

Crump, C.E., Arruda, E., Hayden, F.G., 1993. In vitro inhibitory activity of soluble ICAM-1 for the numbered serotypes of human rhinovirus. Antivir. Chem. Chemother. 4, 323–327.

Gruenberger, M., Pevear, D., Diana, G.D., Kuechler, E., Blaas, D., 1991. Stabilization of human rhinovirus serotype-2 against pH-induced conformational change by antiviral compounds. J. Gen. Virol. 72, 431–433.

Hammar, L., Markarian, S., Haag, L., Lankinen, H., Salmi, A., Cheng, R.H., 2003. Prefusion rearrangements resulting in fusion peptide exposure in Semliki forest virus. J. Biol. Chem. 278, 7189–7198.

He, Y., Lin, F., Chipman, P.R., Bator, C.M., Baker, T.S., Shoham, M., Kuhn, R.J., Medof, M.E., Rossmann, M.G., 2002. Structure of decay-accelerating factor bound to echovirus 7: a virus–receptor complex. Proc. Natl. Acad. Sci. U.S.A. 99, 10325–10329.

Herdy, B., Snyers, L., Reithmayer, M., Hinterdorfer, P., Blaas, D., 2004. Identification of the human rhinovirus serotype 1A binding site on the murine low-density lipoprotein receptor by using human–mouse receptor chimeras. J. Virol. 78, 6766–6774.

Herz, J., Goldstein, J.L., Strickland, D.K., Ho, Y.K., Brown, M.S., 1991. 39-kDa protein modulates binding of ligands to low density lipoprotein receptor-related protein/alpha 2-macroglobulin receptor. J. Biol. Chem. 266, 21232–21238.

Hewat, E., Blaas, D., 2001. Structural studies on antibody interacting with viruses. Curr. Top. Microbiol. Immunol. 260, 29–44.

Hewat, E.A., Neumann, E., Conway, J.F., Moser, R., Ronacher, B., Marlovits, T.C., Blaas, D., 2000. The cellular receptor to human rhinovirus 2 binds around the 5-fold axis and not in the canyon: a structural view. EMBO J. 19, 6317–6325.

Hofer, F., Gruenberger, M., Kowalski, H., Machat, H., Huettinger, M., Kuechler, E., Blaas, D., 1994. Members of the low density lipoprotein receptor family mediate cell entry of a minor-group common cold virus. Proc. Natl. Acad. Sci. U.S.A. 91, 1839–1842.

Konecsni, T., Kremser, L., Snyers, L., Rankl, C., Kilar, F., Kenndler, E., Blaas, D., 2004. Twelve receptor molecules attach per viral particle of

human rhinovirus serotype 2 via multiple modules. FEBS Lett. 568, 99–104.

Lea, S.M., Powell, R.M., McKee, T., Evans, D.J., Brown, D., Stuart, D.I., vanderMerwe, P.A., 1998. Determination of the affinity and kinetic constants for the interaction between the human virus echovirus 11 and its cellular receptor, CD55. J. Biol. Chem. 273, 30443–30447.

Ledford, R.M., Patel, N.R., Demenczuk, T.M., Watanyar, A., Herbertz, T., Collett, M.S., Pevear, D.C., 2004. VP1 sequencing of all human rhinovirus serotypes: insights into genus phylogeny and susceptibility to antiviral capsid-binding compounds. J. Virol. 78, 3663–3674.

Lee, H.J., Yan, Y., Marriott, G., Corn, R.M., 2005. Quantitative functional analysis of protein complexes on surfaces. J. Physiol. 563, 61–71.

Lonberg Holm, K., Noble Harvey, J., 1973. Comparison of in vitro and cell-mediated alteration of a human rhinovirus and its inhibition by sodium dodecyl sulfate. J. Virol. 12, 819–826.

Marlin, S.D., Staunton, D.E., Springer, T.A., Stratowa, C., Sommergruber, W., Merluzzi, V.J., 1990. A soluble form of intercellular adhesion molecule-1 inhibits rhinovirus infection. Nature 344, 70–72.

Marlovits, T.C., Abrahamsberg, C., Blaas, D., 1998a. Soluble LDL minireceptors—Minimal structure requirements for recognition of minor group human rhinovirus. J. Biol. Chem. 273, 33835–33840.

Marlovits, T.C., Abrahamsberg, C., Blaas, D., 1998b. Very-low-density lipoprotein receptor fragment shed from HeLa cells inhibits human rhinovirus infection. J. Virol. 72, 10246–10250.

Marlovits, T.C., Zechmeister, T., Gruenberger, M., Ronacher, B., Schwihla, H., Blaas, D., 1998c. Recombinant soluble low density lipoprotein receptor fragment inhibits minor group rhinovirus infection in vitro. FASEB J. 12, 695–703.

Martin, S., Casasnovas, J.M., Staunton, D.E., Springer, T.A., 1993. Efficient neutralization and disruption of rhinovirus by chimeric ICAM-1/immunoglobulin molecules. J. Virol. 67, 3561–3568.

Mayer, M., Meyer, B., 2001. Group epitope mapping by saturation transfer difference NMR to identify segments of a ligand in direct contact with a protein receptor. J. Am. Chem. Soc. 123, 6108–6117.

Meyer, B., Peters, T., 2003. NMR spectroscopy techniques for screening and identifying ligand binding to protein receptors. Angew. Chem., Int. Ed. 42, 864–890.

Mikhailenko, I., Considine, W., Argraves, K.M., Loukinov, D., Hyman, B.T., Strickland, D.K., 1999. Functional domains of the very low density lipoprotein receptor: molecular analysis of ligand binding and acid-dependent ligand dissociation mechanisms. J. Cell Sci. 112, 3269–3281.

Neubauer, C., Frasel, L., Kuechler, E., Blaas, D., 1987. Mechanism of entry of human rhinovirus 2 into HeLa cells. Virology 158, 255–258.

Neumann, E., Moser, R., Snyers, L., Blaas, D., Hewat, E.A., 2003. A cellular receptor of human rhinovirus type 2, the very-low-density lipoprotein receptor, binds to two neighboring proteins of the viral capsid. J. Virol. 77, 8504–8511.

Nizet, S., Wruss, J., Blaas, D., submitted for publication. A mutation in the first ligand binding repeat of the human very low-density lipoprotein receptor results in high affinity binding of the single V1 module to HRV2. J. Virol.

Nurani, G., Lindqvist, B., Casasnovas, J.M., 2003. Receptor priming of major group human rhinoviruses for uncoating and entry at mild low-pH environments. J. Virol. 77, 11985–11991.

Ohlin, A., Hoover-Litty, H., Sanderson, G., Paessens, A., Johnston, S.L., Holgate, S.T., Huguenel, E., Greve, J.M., 1994. Spectrum of activity of soluble intercellular adhesion molecule-1 against rhinovirus reference strains and field isolates. Antimicrob. Agents Chemother. 38, 1413–1415.

Reithmayer, M., Reischl, A., Snyers, L., Blaas, D., 2002. Species-specific receptor recognition by a minor-group human rhinovirus (HRV): HRV serotype 1A distinguishes between the murine and the human low-density lipoprotein receptor. J. Virol. 76, 6957–6965.

Ronacher, B., Marlovits, T.C., Moser, R., Blaas, D., 2000. Expression and folding of human very-low-density lipoprotein receptor fragments: neutralization capacity toward human rhinovirus HRV2. Virology 278, 541–550.

Rudenko, G., Henry, L., Henderson, K., Ichtchenko, K., Brown, M.S., Goldstein, J.L., Deisenhofer, J., 2002. Structure of the LDL receptor extracellular domain at endosomal pH. Science 298, 2353–2358.

Sakai, J., Hoshino, A., Takahashi, S., Miura, Y., Ishii, H., Suzuki, H., Kawarabayasi, Y., Yamamoto, T., 1994. Structure, chromosome location, and expression of the human very low density lipoprotein receptor gene. J. Biol. Chem. 269, 2173–2182.

Semler, B.L., Wimmer, E. (Eds.), 2002. Molecular Biology of Picornaviruses. ASM Press, Washington D.C., U.S.A., pp. 20036–22904.

Shigeta, S., 1998. Approaches to antiviral chemotherapy for acute respiratory infections. Antivir. Chem. Chemother. 9, 93–107.

Skern, T., Neubauer, C., Frasel, L., Gruendler, P., Sommergruber, W., Zorn, W., Kuechler, E., Blaas, D., 1987. A neutralizing epitope on human rhinovirus type 2 includes amino acid residues between 153 and 164 of virus capsid protein VP2. J. Gen. Virol. 68, 315–323.

Snyers, L., Zwickl, H., Blaas, D., 2003. Human rhinovirus type 2 is internalized by clathrin-mediated endocytosis. J. Virol. 77, 5360–5369.

Strickland, D.K., Kounnas, M.Z., Argraves, W.S., 1995. LDL receptor-related protein: a multiligand receptor for lipoprotein and proteinase catabolism. FASEB J. 9, 890–898.

Verdaguer, N., Fita, I., Reithmayer, M., Moser, R., Blaas, D., 2004. X-ray structure of a minor group human rhinovirus bound to a fragment of its cellular receptor protein. Nat. Struct. Mol. Biol. 11, 429–434.

Vlasak, M., Roivainen, M., Reithmayer, M., Goesler, I., Laine, P., Snyers, L., Hovi, T., Blaas, D., 2005. The minor receptor group of human rhinovirus (HRV) includes HRV23 and HRV25, but presence of a lysine in the VP1 HI loop is not sufficient for receptor binding. J. Virol. 79, 7389–7395.

Xing, L., Casasnovas, J.M., Cheng, R.H., 2003. Structural analysis of human rhinovirus complexed with ICAM-1 reveals the dynamics of receptor-mediated virus uncoating. J. Virol. 77, 6101–6107.

Yin, F.H., Lomax, N.B., 1983. Host range mutants of human rhinovirus in which nonstructural proteins are altered. J. Virol. 48, 410–418.